

1 **Global marine ecosystem response to a strong AMOC**
2 **weakening under low and high future emission**
3 **scenarios**

4 **A. A. Boot¹, J. Steenbeek², M. Coll^{2,3}, A. S. von der Heydt^{1,4}, and H. A.**
5 **Dijkstra^{1,4}**

6 ¹Institute for Marine and Atmospheric research Utrecht, Department of Physics, Utrecht University,
7 Utrecht, the Netherlands

8 ²Ecopath International Initiative (EII) Research Association, Barcelona, Spain

9 ³Department of Marine Renewal Resources, Institute of Marine Science (ICM-CSIC), Barcelona, Spain

10 ⁴Center for Complex Systems Studies, Utrecht University, Utrecht, the Netherlands

11 **Key Points:**

- 12 • Marine ecosystems are negatively affected by a weakening of the Atlantic Merid-
13 ional Overturning Circulation.
14 • Mechanisms involve changes in nutrient transport and subsequent phytoplankton
15 response leading to changes in the food web.
16 • Regional responses depend strongly on shifts in phytoplankton dominance.

Corresponding author: Amber A. Boot, a.a.boot@uu.nl

Abstract

Marine ecosystems provide essential services to the Earth System and society. These ecosystems are threatened by anthropogenic activities and climate change. Climate change increases the risk of passing tipping points; for example, the Atlantic Meridional Overturning Circulation (AMOC) might tip under future global warming leading to additional changes in the climate system. Here, we look at the effect of an AMOC weakening on marine ecosystems by forcing the Community Earth System Model v2 (CESM2) with low (SSP1-2.6) and high (SSP5-8.5) emission scenarios from 2015 to 2100. An additional freshwater flux is added in the North Atlantic to induce an extra weakening the AMOC. In CESM2, the AMOC weakening has a large impact on phytoplankton biomass and temperature fields through various mechanisms that change the supply of nutrients to the surface ocean. We drive a marine ecosystem model, EcoOcean, with phytoplankton biomass and temperature fields from CESM2. In EcoOcean, we see negative impacts in Total System Biomass (TSB), which are larger for high trophic level organisms. The strongest net effect is seen in the high emission scenario, but the effect of the extra AMOC weakening on TSB is larger in the low emission scenario. On top of anthropogenic climate change, TSB decreases by -3.78% and -2.03% in SSP1-2.6 and SSP5-8.5, respectively due to the AMOC weakening. These results show that marine ecosystems will be under increased threat if the AMOC weakens which might put additional stresses on socio-economic systems that are dependent on marine biodiversity as a food and income source.

Plain Language Summary

Marine ecosystems provide essential services to the Earth System and society. These ecosystems are threatened by anthropogenic activities and climate change. Climate change might also lead to a strong weakening of the Atlantic Meridional Overturning Circulation (AMOC). Here, we use a complex Earth System Model and a Marine Ecosystem Model to study how marine ecosystems respond to a strong AMOC weakening in possible future climates (2015-2100) under low and high emission scenarios. The AMOC weakening affects the climate system through various mechanisms that change the supply of nutrients to the surface ocean, affecting the primary production by phytoplankton. We find that the AMOC weakening leads to a decrease in phytoplankton biomass that is larger higher up the food chain. In total, marine ecosystems lose -3.78% and -2.03% of biomass in the low and high emission scenarios respectively. These results show that marine ecosystems will be under increased threat if the AMOC weakens.

Keywords: Atlantic Meridional Overturning Circulation, Climate Change, Marine Ecosystems, Earth System Modelling, Marine Ecosystem Modelling, Tipping Points

1 Introduction

Anthropogenic climate change and other anthropogenic activities, such as overfishing and pollution, are a major threat for marine ecosystems and the services they provide. One of the services marine ecosystems provide is food for (human) consumption. It is estimated that the ocean provides 11% of animal protein that humans consume (Gattuso et al., 2015; FAO, 2022), and besides providing food, it also provides income through the fishery industry. Furthermore, marine ecosystems are estimated to export 11 Gigatonnes of carbon (GtC) each year from the surface to the deep ocean (Sanders et al., 2014), and without this export, atmospheric pCO₂ would be 200-400 ppm higher (Henson et al., 2022; Ito & Follows, 2005). Major changes in marine ecosystems can therefore have an important impact on both socio-economic systems and the climate system, making it very relevant to be able to make reliable projections on the future development of these ecosystems (Lotze et al., 2019; Tittensor et al., 2021).

Evidence of the impact of anthropogenic climate change on marine ecosystems is already apparent. Observations show, for example, a reduction in ocean productivity, changes in food webs, biogeographical shifts, and bleaching of warm water corals (Hoegh-Guldberg & Bruno, 2010; Doney et al., 2012; Gattuso et al., 2015; IPCC, 2022). The effects of climate change can propagate through the ecosystems in bottom-up and top-down direction, causing possible cascades in the ecosystem (Doney et al., 2012; Lotze et al., 2019). Another consequence of climate change is the expansion of hypoxic regions, especially those found along productive regions (Diaz & Rosenberg, 2008; Breitburg et al., 2018), which already has led to mass mortalities (Doney et al., 2012; Sampaio et al., 2021).

It has been suggested that many organisms in the ocean are at a very high risk of impact by climate change by 2100 (Gattuso et al., 2015; Coll et al., 2020), and the function of marine ecosystems is threatened by a possible loss of ecological resilience (Henson et al., 2021). As the climate warms, so does the probability of marine heat waves, which have been shown to have detrimental effects on ecosystems (Smale et al., 2019). Most CMIP6 (Eyring et al., 2016) Earth System Models (ESMs) project a future decrease in Net Primary Production (NPP). However, the intermodel spread in these projections is large and this spread has even increased compared to CMIP5 ESMs (Kwiatkowski et al., 2020; Tagliabue et al., 2021; Henson et al., 2022). Marine Ecosystem Models (MEMs) using input from two CMIP6 ESMs, project a decrease in Total System Biomass (TSB) in both a low and a high emission scenarios even though there is substantial spread in NPP in the ESMs (Tittensor et al., 2021).

Climate warming is not only a risk to marine ecosystems, it might also lead to tipping in the Earth System (Lenton et al., 2008; McKay et al., 2022). Passing a tipping point is a serious risk since the consequences of tipping are irreversible and can therefore be disastrous. A major tipping element in the ocean is the Atlantic Meridional Overturning Circulation (AMOC). The AMOC potentially has two stable states: an on-state reflecting the current AMOC regime with a strong circulation, and an off-state reflecting a weak or collapsed AMOC (Weijer et al., 2019). Tipping of the AMOC would lead to several changes in the Earth System affecting the entire globe. In the on-state the AMOC is responsible for a net transport of heat from the Southern Hemisphere across the equator to the Northern Hemisphere of 0.5 PW (Liu et al., 2017; Forget & Ferreira, 2019) thereby strongly influencing observed surface air temperature patterns. An AMOC collapse is expected to result in a cooling in the Northern Hemisphere and warming in the Southern Hemisphere, a southward shift of the Intertropical Convergence Zone (ITCZ), and a strengthening of the trade winds (van Westen & Dijkstra, 2023a; Orihuela-Pinto et al., 2022; Caesar et al., 2018). As a response to the cooling, Arctic sea-ice extent is expected to increase under AMOC weakening or collapse. Besides the direct changes in advection due to an AMOC collapse, an AMOC weakening can also change important ocean characteristics such as the stratification and upwelling rates. Several studies have shown the impact this can have on the marine carbon cycle and the uptake capacity of the ocean (Zickfeld et al., 2008; Boot, von der Heydt, & Dijkstra, 2024). The changes in stratification and upwelling rates are specifically interesting for marine ecosystems, and through these processes, an AMOC weakening can impact marine primary productivity (Schmittner, 2005). The changes in ocean circulation also alter the connectivity in the ocean which can be relevant for environmental niches of plankton species, especially when their thermal constraints are taken into account (Manral et al., 2023). This provides a bottom-up control on marine ecosystems potentially threatening important ecosystem services and a pathway of cascading tipping from the physical climate system into marine ecosystems (Brovkin et al., 2021).

There are studies that suggest that the AMOC has been weakening over the past century (Caesar et al., 2018), and that the AMOC might tip between 2025 and 2095 (Ditlevsen & Ditlevsen, 2023). These studies are based on uncertain proxy data and are contested by some other studies (Worthington et al., 2021). However, a recent study using a physics

118 based early warning signal shows that the AMOC is indeed on tipping course (van Westen
 119 et al., 2024). In CMIP6, the models show a consistent weakening of the AMOC across
 120 almost all emission scenarios, but no AMOC collapse is simulated up to 2100 (Weijer et
 121 al., 2020). However, this might be explained by the fact that the CMIP6 models are bi-
 122 ased towards a too stable AMOC (van Westen & Dijkstra, 2023b) and might therefore
 123 underestimate the probability of a collapse.

124 In this study, we examine the impact of a strong AMOC weakening on marine ecosys-
 125 tems under anthropogenic climate change. We do this by analysing several simulations
 126 of the Community Earth System Model v2 (CESM2; Danabasoglu et al., 2020) where
 127 we use both a low and a high emission scenario, and simulations where we artificially weaken
 128 the AMOC by applying a surface freshwater flux to the North Atlantic Ocean. Since the
 129 ecosystem component in CESM2 is limited to three different phytoplankton groups and
 130 only one zooplankton group, we use the marine ecosystem model (MEM) EcoOcean (Coll
 131 et al., 2020) to simulate more detailed ecosystem dynamics. We force EcoOcean, a MEM
 132 part of FishMIP (Tittensor et al., 2018, 2021), with the output of the CESM2 simula-
 133 tions. Our results demonstrate the far reaching effects that a weakening of the AMOC
 134 can have on the marine ecosystem.

135 2 Methods

136 2.1 Earth System Model

137 The Community Earth System Model v2 (CESM2) is a state-of-the-art Earth Sys-
 138 tem Model that is part of CMIP6. It has modules that represent the atmosphere (the
 139 Community Atmosphere Model v6), the land (the Community Land Model v5; Lawrence
 140 et al., 2019), sea ice (CICE5; Hunke et al., 2015), and the ocean (the Parallel Ocean Pro-
 141 gram v2, POP2; Smith et al., 2010) including ocean biogeochemistry (the Marine Bio-
 142 geochemical Library, MARBL; Long et al., 2021). In this study we use the default CMIP6
 143 version of CESM2, meaning that ice sheets and vegetation type are prescribed. All mod-
 144 els are run on a nominal resolution of 1° , but the exact grid differs between the mod-
 145 ules. Important for this study are the ocean modules POP2 and MARBL. These are both
 146 run on a displaced grid with a pole in Greenland. The vertical grid consists of 60 dif-
 147 ferent layers with a thickness of 10 m in the top 150 m, after which the layer thickness
 148 increases to 250 m at 3500 m depth, staying constant up to the maximum ocean depth
 149 of 5500 m.

150 The ocean biogeochemistry module in CESM2 is MARBL (Long et al., 2021), which
 151 is an updated version of the Biogeochemical Elemental Cycling model (BEC; J. K. Moore
 152 et al., 2001, 2004, 2013; C. M. Moore et al., 2013). MARBL resolves three explicit phy-
 153 toplankton types: diatoms, diazotrophs and small phytoplankton. Calcification is mod-
 154 elled implicitly as part of the small phytoplankton group using a variable rain ratio. Phy-
 155 toplankton growth is co-limited by light and by silica (Si), phosphorus (P), nitrogen (N)
 156 and iron (Fe). Diatoms are the only group that can be limited by Si, and diazotrophs
 157 are nitrogen fixers and therefore not limited by N. However, diazotrophs are severely tem-
 158 perature limited if sea surface temperatures (SSTs) are below 15°C . The three phyto-
 159 plankton types are grazed upon by one zooplankton group that, through differential graz-
 160 ing, implicitly represents multiple zooplankton groups (e.g. micro- and meso zooplank-
 161 ton). Both phyto- and zooplankton have a linear mortality formulation and for zooplank-
 162 ton a parametrized loss term is included that represents higher order trophic grazing.
 163 All primary production and consumption takes place in the top 150 m of the water col-
 164 umn.

165 We use the same simulations that are presented in Boot, von der Heydt, and Di-
 166 jkstra (2024) where the marine and terrestrial carbon cycle response to a strong AMOC
 167 weakening is studied. For a more thorough discussion on the simulations we refer the reader

168 to Boot, von der Heydt, and Dijkstra (2024). We use emissions of two different scenar-
 169 ios: a low emission scenario SSP1-2.6 (from here on also referred to as 126), and a high
 170 emission scenario SSP5-8.5 (585). For each emission scenario there is a control (CTL)
 171 simulation where we force the model only with the emissions of the scenarios, and a sim-
 172 ulation where we also apply a uniformly distributed freshwater flux in the North Atlantic
 173 Ocean between 50°N and 70°N at a constant rate of 0.5 Sv throughout the entire sim-
 174 ulation (HOS simulations). We will refer to the simulations by combining the type and
 175 emission scenario, e.g. CTL-585 and HOS-126. All simulations are run from 2015 to 2100
 176 and are initialized from the emission driven NCAR CMIP6 historical ('esm-hist') sim-
 177 ulation (Danabasoglu, 2019).

178 2.2 Marine ecosystem model

179 We use EcoOcean v2 (Coll et al., 2020), an updated version of EcoOcean v1 (Christensen
 180 et al., 2015), which is one of the global, spatiotemporal explicit MEMs contributing to
 181 FishMIP (Tittensor et al., 2018, 2021). EcoOcean was originally developed to assess the
 182 impact of management strategies on the supply of seafood on a global scale. It is a 2D
 183 model with a horizontal resolution of 0.25 to 1° and simulates the time period 1950 to
 184 2100 using monthly time steps. The EcoOcean framework combines several models which
 185 can be divided into three main components: (1) a component for marine biogeochem-
 186 ical processes and primary production, (2) a food web component that includes a dy-
 187 namic niche model and species movement, and (3) a component simulating fisheries. Pre-
 188 viously, EcoOcean was driven by simulations of the IPSL (using PISCES for ocean bio-
 189 geochemistry; Boucher et al., 2020) and the GFDL (using COBALT for ocean biogeo-
 190 chemistry; Dunne et al., 2020) Earth System Models (Tittensor et al., 2018, 2021). In
 191 this study, we use the output of MARBL from the CESM2 simulations described in the
 192 previous section for component (1), and to match the resolution of CESM2, EcoOcean
 193 is used with a 1° resolution. We will not use active fisheries in this study and therefore
 194 component (3) is switched off. For a more thorough discussion on EcoOcean and the sen-
 195 sitivity of the model formulation, we refer the reader to Christensen et al. (2015) (v1)
 196 and Coll et al. (2020) (v2), and references therein.

197 The ecosystem module in EcoOcean simulates 52 different functional groups rep-
 198 resenting over 3400 individual species. Species are grouped together when biological and
 199 ecological traits are similar. The functional groups range from bacteria, plankton, dif-
 200 ferent groups of fish, to marine mammals and birds. The different fish groups are dif-
 201 ferentiated on size (small: < 30 cm, medium: 30-90cm, large: > 90 cm), and grouped
 202 on, for example, where they live in the water column, i.e. pelagics, demersals, bathypelag-
 203 ics, bathydemersals, benthopelagics, reef fishes, sharks, rays and flat fishes. For a com-
 204 plete list of all functional groups, see the Supplementary Table 1 from Coll et al. (2020).

205 The food web model in EcoOcean is based on the 'Foraging Arena Theory' (Walters
 206 & Juanes, 1993; Ahrens et al., 2012), and the relative habitat capacity is determined us-
 207 ing the Habitat Foraging Capacity Model (HFCM) (Christensen et al., 2014). Based on
 208 local predation risks and food availability, groups can move across spatial cells (Walters
 209 & Juanes, 1993; Martell et al., 2005; Christensen et al., 2014). The cell suitability in the
 210 HFCM is dependent on species native ranges, foraging capacity related to affinities for
 211 specific habitat distributions and types, and the response of the functional groups to en-
 212 vironmental drivers.

213 The three phytoplankton groups simulated in the CESM2 are used to drive distri-
 214 butions and magnitude of corresponding planktonic groups in EcoOcean, and three dif-
 215 ferent temperature fields in the CESM2 are used to drive the EcoOcean HFCM. One tem-
 216 perature field is averaged over the top 150 m, a second is depth averaged over the whole
 217 column, and the third represents bottom temperatures. Recall that the CESM2 simu-
 218 lations start in 2015 initialized from NCAR CMIP6 historical simulations (Danabasoglu,

219 2019). To run EcoOcean accurately, it needs to be calibrated to observations in the pe-
 220 riod 1950 to 2015. To be able to do this, we need also input variables for this period. The
 221 CESM2 simulations used in this study start at 2015 and are branched off from histori-
 222 cal CMIP6 CESM2 simulations performed by NCAR. Unfortunately, not all necessary
 223 input variables to calibrate EcoOcean are available for the period 1950 to 2015 from these
 224 simulations and therefore we can not accurately calibrate EcoOcean to observations. We
 225 will therefore use relative changes in biomass B , defined as $\frac{B(t=2099)-B(t=2015)}{B(t=2015)} \times 100\%$,
 226 to assess the effect of the AMOC weakening on marine biomass. To spin up EcoOcean,
 227 we repeat the 2015 forcing of the CESM2 simulations in EcoOcean until a quasi-steady
 228 state is reached to replace the 1950-2015 calibration period. We look at three different
 229 aggregated groups of marine biomass: Total system biomass (TSB), total consumer biomass
 230 (TCB), and total commercial biomass (COM). For a definition of the three groups in EcoOcean
 231 see the supplementary material (Supplementary Table 1) of Coll et al. (2020).

232 3 Results

233 3.1 CESM2 Climate response

234 In both emission scenarios, the greenhouse gas emissions cause an increase in CO_2
 235 concentration and warming. In CTL-585, CO_2 concentrations increase up to 1094 ppm
 236 in 2100, whereas CTL-126 has a maximum concentration in 2055 after which it decreases
 237 to 434 ppm due to negative emissions (Fig. 1a). The difference in atmospheric pCO_2 also
 238 result in a different Global Mean Surface Temperature (GMST), with around 5°C warm-
 239 ing in CTL-585, and 1°C warming in CTL-126 (Fig. 1b). The forcing of the model causes
 240 a near linear weakening of the AMOC of around 50% for both emission scenarios, with
 241 a 2 Sv stronger weakening in CTL-585 (Fig. 1c). In the HOS simulations, the AMOC
 242 weakens much faster and stronger compared to the CTL simulations (Fig. 1c, f) as a re-
 243 sponse to the freshwater forcing. The maximum difference between the HOS and CTL
 244 simulations is around 8 Sv in the 2040's, and then decreases again (Fig. 1f). Due to the
 245 AMOC weakening, GMST warming is reduced following a similar trend as the reduc-
 246 tion in AMOC strength (Fig. 1e). Also the spatial pattern of warming is affected by the
 247 AMOC weakening. The reduced northward heat transport in the HOS simulations causes
 248 relative cooling of both surface air temperature (SAT; Fig. S1) and sea surface temper-
 249 ature (SST; Fig. 2) in the Northern Hemisphere and relative warming in the Southern
 250 Hemisphere compared to the CTL simulations. The response in atmospheric pCO_2 to
 251 the hosing is small (Fig. 1d) related to many compensating effects within the carbon cy-
 252 cle (see Boot, von der Heydt, & Dijkstra, 2024).

253 The different temperature distribution in the HOS simulations compared to the CTL
 254 simulations causes atmospheric adjustments resulting in a southward shift of the ITCZ
 255 (Fig. S2), and a strengthening of the Northern Hemispheric trade winds (Fig. S3), both
 256 of which have an important influence on the surface stratification of the ocean (Fig. S4)
 257 and upwelling rates (Fig. S5). As a consequence to the relatively cooler Northern Hemi-
 258 sphere, Arctic sea-ice extent increases in both HOS simulations compared to their re-
 259 spective CTL simulations (Fig. S6). At the end of the simulation, the sea ice extent in
 260 HOS-126 is actually larger in 2100 compared to 2015, and also much larger compared
 261 to CTL-126 (Fig. S6c). In HOS-585 the strong warming still results in a much reduced
 262 Arctic sea-ice cover. However, the melting of the sea ice is much slower and, compared
 263 to CTL-585, HOS-585 also has more ice in 2100 (Fig.S6f).

264 3.2 CESM2 biogeochemical response

265 The changes in, for example, stratification and upwelling rates influence the nu-
 266 trient concentrations in the euphotic zone of the ocean. In the CTL simulations, phos-
 267 phate (PO_4^{3-}) concentrations decrease in the surface ocean almost everywhere (Fig. S7).
 268 The strongest responses are seen in the North Atlantic and Arctic Ocean, and in the East-

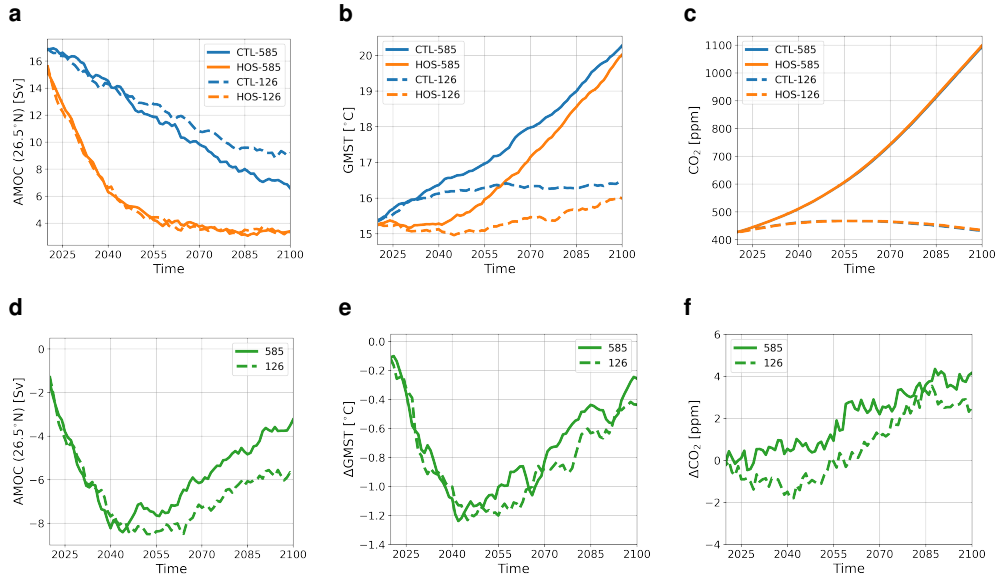


Figure 1. (a) Atmospheric CO₂ concentration in ppm. (b) GMST in °C. (c) AMOC strength at 26.5°N in Sv. In (a-c) blue lines represent the control (CTL) simulations, and orange lines the HOS simulations. (d-f) as in (a-c) but for the difference between the HOS simulations and the control simulations. In all subplots dashed lines represent SSP1-2.6 (126) and solid lines SSP5-8.5 (585). Results are smoothed with a 5 year moving average and represent the period 2020-2100.

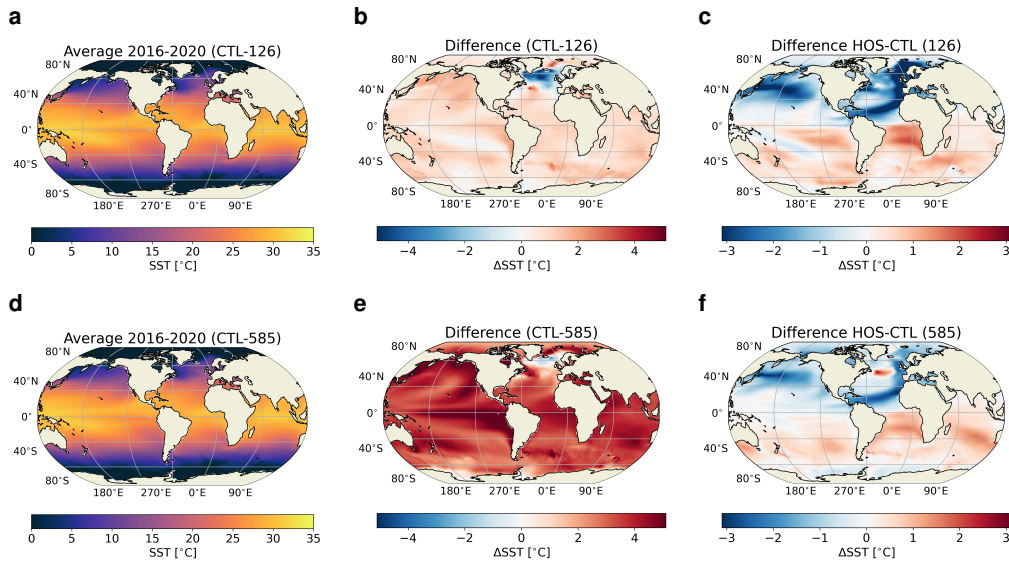


Figure 2. Sea Surface Temperature (SST) in °C for: (a) CTL-126 averaged over 2016-2020, (b) the average over 2016-2020 subtracted from the average over 2095-2099 in CTL-126, (c) CTL-126 subtracted from HOS-126 averaged over 2095-2099, and (d-f) as in (a-c) but for CTL-585 and HOS-585.

ern Equatorial and South Pacific Ocean, with in all regions a stronger response in CTL-585 compared to CTL-126. Nitrate (NO_3^-) concentrations do not decrease everywhere in the ocean in the CTL simulations, but just as with PO_4^{3-} , the strongest responses are seen in the North Atlantic, and Eastern Equatorial and South Pacific Ocean. (Fig. 3) There are also relatively strong decreases in the Northwestern Pacific Ocean. Just as for PO_4^{3-} the response is stronger in CTL-585 compared to CTL-126. Silicate (SiO_3^{2-}) shows a very similar response in the CTL simulations as NO_3^- , except in the Southern Ocean south of 40°S where a large decrease is simulated for both emission scenarios (Fig. S8). The response of iron (Fe) is slightly different compared to the other nutrients in the CTL simulations (Fig. S9). Large increases are seen in the Russian Arctic Ocean, along the equator, and in the subtropical North Atlantic Ocean. The largest decreases are seen in the rest of the Arctic Ocean, and the Northern Indian Ocean. The response in CTL-585 is typically a bit stronger compared to CTL-126, especially in the Eastern Equatorial Pacific, and south of Madagascar.

As a response to the AMOC weakening, there are additional large decreases in PO_4^{3-} concentrations for both scenarios in the North Equatorial Pacific, the Eastern Equatorial and Southern Atlantic, especially in the Benguela Upwelling System. Large increases are seen in the Canary Upwelling System (Fig. S7). The response to the AMOC weakening is very similar for NO_3^- compared to PO_4^{3-} except in the Arctic Ocean, where in the HOS simulations NO_3^- concentrations increase (Fig. 3). The response of SiO_3^{2-} to the AMOC weakening in the HOS simulations is also very similar to the responses in PO_4^{3-} and NO_3^- (Fig. S8). Again the response of Fe to the AMOC weakening in the HOS simulations compared to the CTL simulations differs from the other nutrients (Fig. S9). Most of the Southern Hemisphere sees a relative reduction in surface Fe concentrations except the South Atlantic and a small part of the South Pacific between 0 and 15°S , which actually sees some of the strongest increases relative to the CTL simulations. The North Pacific Ocean also sees relative increases, just as some parts of the North Atlantic and Arctic Ocean. In the Atlantic Ocean between 0 and 25°N , large relative decreases are seen. The two emission scenarios show very similar responses to the AMOC weakening except for some regional differences, such as in the Indian Ocean, and North Atlantic Ocean.

The response of the nutrients to the greenhouse gas emissions induced climate change in the CTL simulations result in changes in Net Primary Production (NPP; Fig. 4) and Export Production (EP; Fig. S10). NPP decreases in the North Atlantic Ocean (north of 30°N) as a response to the greenhouse gas emissions in both scenarios. In CTL-585 there are also large anomalies in the Eastern Equatorial Pacific (positive) and Western Equatorial Pacific (negative). In response to the AMOC weakening, we mostly see changes in the Atlantic basin (decrease) and in the Northeastern Equatorial Pacific (increase). In the Atlantic, the subtropical gyres (north and south) and the Benguela Upwelling System there is a large decrease in NPP, and in the Canary Upwelling System and along the North Equatorial Current there is a large increase in NPP in the HOS simulations compared to the CTL simulations.

The changes in primary productivity are also related to changes in biomass of the three phytoplankton groups. In the CTL simulations, the response of the diazotrophs (Fig. S13) can be mostly explained by the poleward shift of the 15°C isotherm (SST) as a response to the warming. We can see bands of strong increases of biomass along this isotherm with a stronger and more poleward increase in CTL-585 due to the larger warming in this simulation. In the HOS simulations, the 15°C isotherm shifts further poleward in the Southern Hemisphere due to the increased warming observed there compared to the CTL simulations. In the Northern Hemisphere, however, we see in the HOS simulations that this isotherm does not shift poleward, except for the North West Atlantic basin in HOS-585. Also diazotroph biomass decreases along the Iberian peninsula.

The diatoms show large decreases in the subpolar North Atlantic Ocean in the CTL simulations, and in CTL-585 areas with strong increases in the Southern Ocean (Fig. S14).

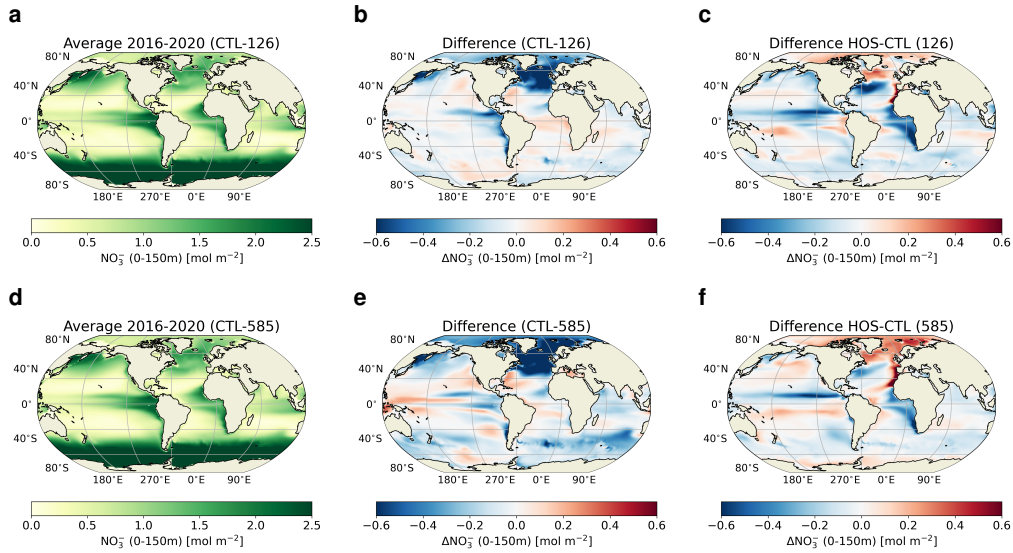


Figure 3. Nitrate (NO_3^-) concentrations integrated over the top 150 m in mol m^{-2} for: (a) CTL-126 averaged over 2016-2020, (b) the average over 2016-2020 subtracted from the average over 2095-2099 in CTL-126, (c) CTL-126 subtracted from HOS-126 averaged over 2095-2099, and (d-f) as in (a-c) but for CTL-585 and HOS-585.

322 This decrease in the subpolar North Atlantic can partly be explained by increased nu-
 323 trient limitation due to reduced entrainment of nutrients from subsurface waters related
 324 to shallow mixed layer depth in this region. As the diatom biomass decreases, the light
 325 limitation for the small phytoplankton is lifted and they are able to outcompete the di-
 326 atoms resulting in a shift of phytoplankton functional type in this region (Boot et al.,
 327 2023). In the HOS simulations, the largest changes in small phytoplankton occur very
 328 locally, i.e. between the subtropical and subpolar gyre in the North Atlantic, the Canary
 329 Upwelling System, the Benguela Upwelling System, around Tasmania and the equatori-
 330 al West Pacific. In the CTL simulations, the small phytoplankton generally perform
 331 well in regions where diatom biomass decreases and vice versa, which is also the case in
 332 the HOS simulations (Fig. S15).

333 3.3 Role of AMOC weakening in CESM2

334 3.3.1 Temperature fields

335 The Habitat Foraging Capacity Model (HFCM) in EcoOcean is driven by three
 336 different temperature fields: the temperature averaged over the top 150 m (Fig. S16),
 337 the temperature averaged over the entire water column (Fig. S17), and the bottom tem-
 338 perature (Fig. S18). The mean temperature of the top 150 m shows a different pattern
 339 than the SSTs (Fig. 2) as a response to the AMOC weakening. The top 150 m in the
 340 Subpolar North Atlantic and Arctic Ocean contains more heat in the HOS simulations
 341 compared to the CTL simulations. The Subtropical North Atlantic Ocean cools, whereas
 342 the South Atlantic warms. In the Indian and Southern Ocean, the northern Subtropi-
 343 cal and southern Subpolar Pacific we see warming, and in the northern Subpolar and
 344 southern Subtropical Pacific we see cooling. Bottom temperatures show the largest re-
 345 sponse in the shallow regions. Generally these regions cool in the Northern Hemisphere
 346 and warm in the Southern Hemisphere. A major exception is the Arctic Ocean and some

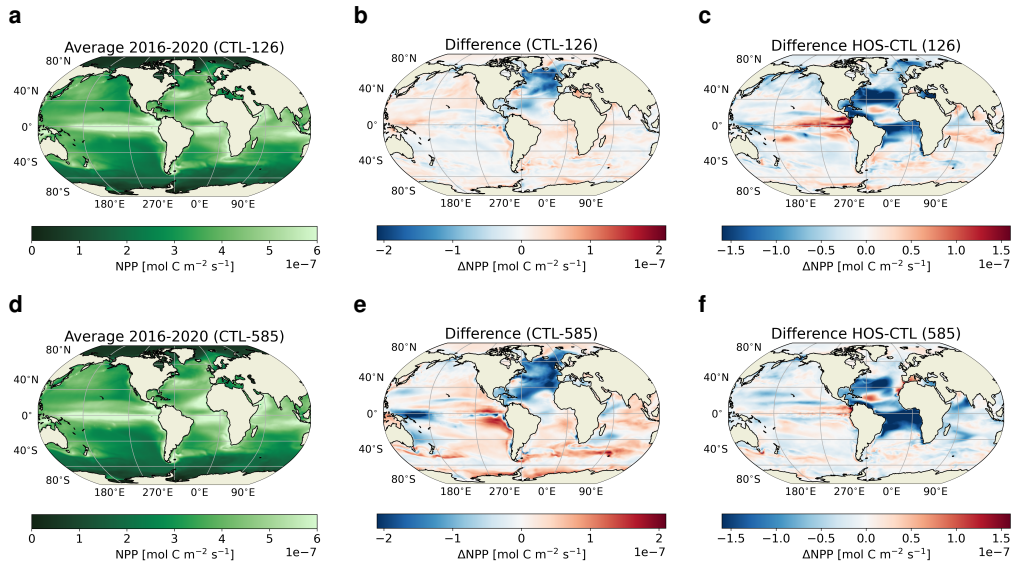


Figure 4. Net Primary Production integrated over the top 150 m in $\text{mol C m}^{-2} \text{s}^{-1}$ for: (a) CTL-126 averaged over 2016-2020, (b) the average over 2016-2020 subtracted from the average over 2095-2099 in CTL-126, (c) CTL-126 subtracted from HOS-126 averaged over 2095-2099, and (d-f) as in (a-c) but for CTL-585 and HOS-585.

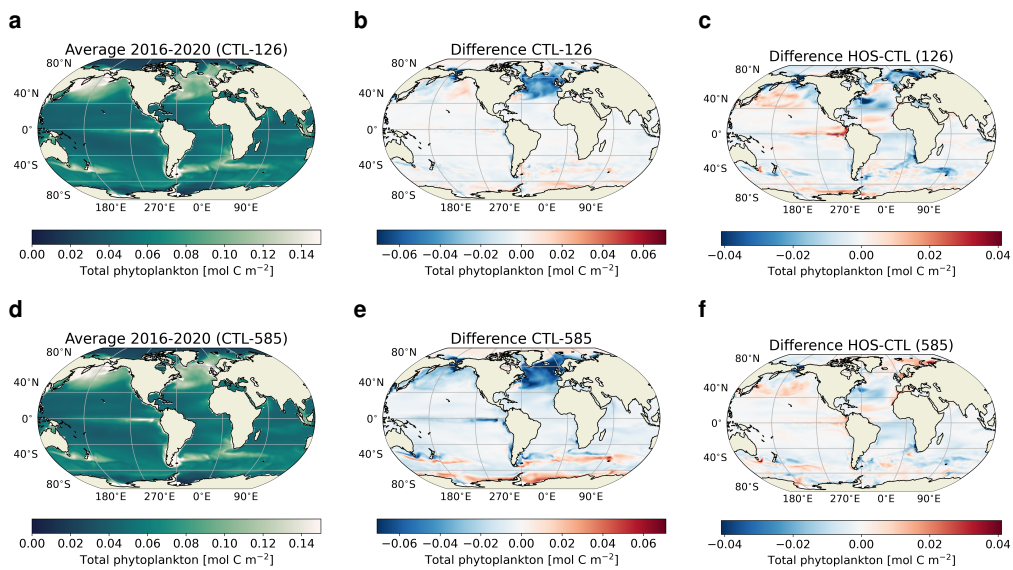


Figure 5. Total phytoplankton biomass integrated over the top 150 m in mol C m^{-2} for: (a) CTL-126 averaged over 2016-2020, (b) the average over 2016-2020 subtracted from the average over 2095-2099 in CTL-126, (c) CTL-126 subtracted from HOS-126 averaged over 2095-2099, and (d-f) as in (a-c) but for CTL-585 and HOS-585.

347 regions in the Subpolar North Atlantic Ocean that warm strongly. The column averaged
 348 water temperature follows generally the trend in the top temperature, except in the shall-
 349 low regions. Here the trends are more similar to the trends seen in the bottom temper-

350 ature. The warming in the Subpolar North Atlantic and Arctic Ocean are related to the
 351 insulating effects of sea ice. The warming in the Northern Subtropical and cooling in the
 352 Southern Subtropical Pacific Ocean are related to the stratification. Increased stratifi-
 353 cation north of the equator results in less upward mixing of cool subsurface waters while
 354 south of the equator the opposite occurs. The other regions follow the trends generally
 355 also observed in SSTs and SATs and are thus related to the forcing at the surface ocean.

356 **3.3.2 Diazotrophs**

357 The extent of the diazotrophs (Fig. S13) is limited by the 15°C SST (Fig. 2) isotherm
 358 as described earlier. The additional AMOC weakening in the HOS simulations affects
 359 the location of this isotherm on top of the climate change signal. In the HOS simulations
 360 in the Southern Hemisphere it shifts poleward due to the additional warming there, and
 361 in the North Pacific it shifts equatorward due to the relative cooling. In the North At-
 362 lantic the response is a bit different, and also differs between the emission scenarios. In
 363 the SSP1-2.6 scenario it shifts equatorward with a stronger response on the eastern side
 364 of the basin. On the eastern side of the basin water from the subpolar North Atlantic
 365 is advected southward. Since the subpolar region cools strongly due to the AMOC weak-
 366 ening, these water masses are relatively cool causing the relative cooling observed around
 367 the Iberian peninsula. In SSP5-8.5 this response on the eastern side of the basin is also
 368 seen, but on the western side we see a poleward increase of the diazotrophs because of
 369 a patch of surface ocean around 50°N that warms. This warming is caused by a south-
 370 ward shift of the North Atlantic Current in CTL-585 that is not found in to HOS-585
 371 and the SSP1-2.6 simulations (Fig. S19).

372 **3.3.3 Diatoms**

373 For the diatoms (Fig. S14) there are a few regions that stand out in the HOS sim-
 374 ulations compared to the CTL simulations. In the Western North Pacific Ocean, East-
 375 ern Equatorial Pacific Ocean, and North Subpolar Atlantic Ocean there are relative in-
 376 creases in diatom biomass for both emission scenarios over a relatively large area. Lo-
 377 cally, there are also relative increases around Tasmania and in the Canary Upwelling Sys-
 378 tem. The largest decreases are found in the extension of the Gulf Stream and in the Benguela
 379 Upwelling System.

380 The increases of diatoms in the Canary Upwelling System can be attributed to the
 381 strengthened trade winds (Fig. S3) in the HOS simulations which increase upwelling (Fig.
 382 S5) in this region. This upwelling supplies more nutrients to the surface ocean driving
 383 an increase in NPP in this region (Figs. 4 and S11). Also the increases in the Equator-
 384 ial Pacific can be related to the AMOC weakening. The southward shift of the ITCZ
 385 decreases the stratification north of the equator (Fig. S4) because the freshwater flux
 386 at the surface ocean decreases (Fig. S3). The weaker stratification leads to deeper mixed
 387 layer depths (Fig. S20) and more entrainment of nutrients from the subsurface ocean.
 388 The increased availability of nutrients in the surface ocean drives an increase in diatom
 389 productivity and biomass (Figs. S11 and S14). The response in the North Subpolar At-
 390 lantic Ocean, where we see a region with a relative increase of diatoms biomass (in the
 391 gyre), and a region with a relative decrease of diatom biomass, can be explained by the
 392 NO_3^- concentrations (Fig. 3). In the CTL simulations, NO_3^- decreases in the subpolar
 393 region, increasing the nitrogen limitation of all phytoplankton in this region. Under in-
 394 creased nutrient stress, small phytoplankton are able to outcompete the diatoms (Boot
 395 et al., 2023). In the HOS simulations, the NO_3^- concentrations increase in the subpo-
 396 lar gyre, and decrease in the extension of the Gulf Stream, and the diatoms respond, by
 397 increasing their mass in the subpolar gyre, and decreasing their mass in the extension
 398 of the Gulf Stream compared to the CTL simulations. The NO_3^- concentrations in the
 399 extension of the Gulf Stream decrease because the weaker Gulf Stream transports less
 400 nutrients northwards, which is directly related to the weakening of the AMOC. Diatom

Table 1. Relative change in % of different total phytoplankton biomass, biomass of the three phytoplankton groups in CESM2, Total System Biomass, Total Consumer Biomass and total commercial biomass in EcoOcean in the year 2099 for the four different simulations and the difference between the HOS and CTL simulations (fourth column for SSP1-2.6 and last column for SSP5-8.5). Relative change is defined as the difference in biomass between 2099 and 2015 divided by the biomass in 2015.

Group	CTL-126	HOS-126	Δ -126	CTL-585	HOS-585	Δ -585
Total phytoplankton biomass	-3.99	-7.41	-3.42	-12.71	-13.56	-0.85
Small phytoplankton biomass	5.91	5.38	-0.53	-5.94	-9.00	-3.06
Diatom biomass	-13.96	-20.98	-7.02	-21.62	-20.44	1.18
Diazotroph biomass	3.81	3.03	-0.78	11.15	11.75	0.60
Total System Biomass	-1.41	-5.20	-3.78	-11.29	-13.33	-2.03
Total Consumer Biomass	-1.64	-5.92	-4.28	-12.49	-14.80	-2.31
Commercial species	-1.48	-4.92	-3.43	-12.75	-15.51	-2.76

401 biomass decreases in the Benguela Upwelling System because the advection of Si through
402 the Aghulas leakage reduces.

403 **3.3.4 Small Phytoplankton**

404 Generally, small phytoplankton (Fig. S15) respond opposite to the diatoms in the
405 HOS simulations compared to the CTL simulations. This is because the diatoms and small
406 phytoplankton are generally competing for the same nutrients. Due to the AMOC weak-
407 ening, locally the environmental conditions can change that can either favor the diatoms
408 or the small phytoplankton. For example, the reduced Si concentrations in the Benguela
409 Upwelling System (Fig. S8) causes the small phytoplankton to become dominant in this
410 region since they are able to outcompete the diatoms.

411 **3.3.5 Total phytoplankton biomass**

412 The change in total phytoplankton biomass (Fig. 5) is generally the combined sig-
413 nal of the changes observed in diatom biomass and small phytoplankton biomass. There
414 are, however, some regions where diatoms replace small phytoplankton or vice versa. In
415 these regions the signal observed in the diatoms is generally dominant, but not every-
416 where (e.g. in the Fram Strait in SSP1-2.6). For each plankton type and the total phy-
417 toplankton biomass, the relative change over the simulation in % is shown in Table 1 for
418 the entire ocean, and in Table S1 per region in the ocean.

419 **3.4 EcoOcean: ecosystem response**

420 There is a clear difference in the response in EcoOcean to the emission scenarios.
421 In CTL-126, total system biomass (TSB) decreases by 1.41%, total consumer biomass
422 (TCB) by 1.64% and commercial species by 1.48% (Table 1). In CTL-585, the decreases
423 are much stronger: TSB decreases by 11.29%, TCB by 12.49% and commercial biomass
424 by 12.75% (Table 1).

425 The response to the greenhouse gas emissions is different per region (Table 2). In
426 both CTL-126 and CTL-585 the ocean around Antarctica ($66^{\circ}\text{S} - 90^{\circ}$) gain the most
427 TSB (37.17% and 47.3%, respectively), and the subpolar North Atlantic and Pacific Ocean
428 lose the most TSB (16.9% and 33.64% for the Atlantic and 12.92% and 25.98% for the

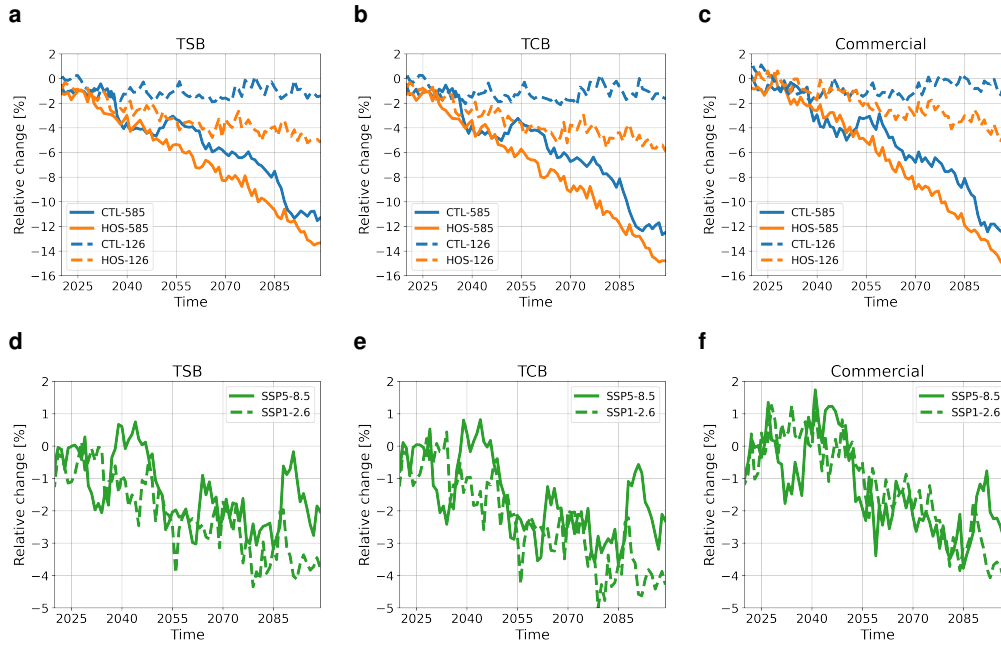


Figure 6. Relative changes in % in the CTL and HOS simulations (top row) and the difference between the two (bottom row) for Total System Biomass (TSB; a, d), Total Consumer Biomass (TCB; b, e), and Commercial species (c, f). Dashed lines represent SSP1-2.6 and solid lines SSP5-8.5. Blue represent the CTL simulations, orange the HOS simulations, and green the difference between the two (HOS minus CTL).

429 Pacific). An important difference between the emission scenarios is how the ecosystems
 430 develop in the Arctic Ocean ($66^{\circ}\text{N} - 90^{\circ}\text{N}$). In CTL-126 the Arctic Ocean loses 9.34%
 431 in TSB, while in CTL-585 we see an increase of 12.71%, which can be explained by look-
 432 ing at the sea-ice cover (Fig. S6). In CTL-585 most sea ice disappears which boosts NPP
 433 (Fig. 4) in this region providing the ecosystem with biomass to feed upon in a bottom
 434 up manner.

435 The effect of the strong AMOC weakening in HOS-126 results in a decrease in biomass
 436 with respect to CTL-126. TSB decreases with 3.78% with respect to CTL-126 and 5.20%
 437 in total (Table 1). The largest responses are seen in the Arctic Ocean, subpolar and sub-
 438 tropical ($15^{\circ}\text{N}-40^{\circ}\text{N}$) North Atlantic Ocean (30.45, 15.22, and 13.24% decrease in TSB
 439 with respect to CTL-126; Table 2). Compared to SSP1-2.6, the relative effect of the AMOC
 440 weakening is lower in SSP5-8.5 which is related to the much stronger climate forcing in
 441 the high emission scenario. TSB decreases with 2.03% with respect to CTL-585 and 13.33%
 442 in total. The largest response in TSB over time is seen in the Arctic Ocean and the sub-
 443 polar North Atlantic, but, just as with the AMOC and GMST difference (Fig. 1), the
 444 difference becomes smaller over time. In 2100, the regions with the largest response in
 445 TSB are the oceans around Antarctica (an increase of 12.97% with respect to CTL-585),
 446 and in the Atlantic north of 15°S (a decrease of 6.38% around the equator, 5.9% in the
 447 subtropical gyre and 6.87% in the subpolar gyre (Fig. 7) with respect to CTL-585).

448 TCB and commercial species show similar results as for TSB, but the global re-
 449 sponse is slightly stronger (except for commercial species in HOS-126), i.e. there is a larger
 450 decrease in biomass of TCB and commercial species compared to TSB (Fig. 6). Region-
 451 ally, the response is generally also similar to the results for TSB, but whether the response

Table 2. Relative change in % of Total System Biomass (TSB), Total Consumer Biomass (TCB) and total commercial biomass (COM) in 2099 for the difference between the HOS and CTL simulations for different regions in the ocean. Relative change is defined as in the main text as the difference in biomass between 2099 and 2015 divided by the biomass in 2015.

Region		TSB		TCB		COM	
		Δ -126	Δ -585	Δ -126	Δ -585	Δ -126	Δ -585
Arctic Ocean	66°N - 90°N	-30.45	0.20	-31.58	0.19	-16.6	-1.18
Atlantic Ocean	40°N - 66°N	-15.22	-6.87	-15.88	-7.23	-17.1	-11.39
	15°N - 40°N	-13.24	-5.90	-14.46	-6.46	-15.04	-6.70
	15°S - 15°N	-5.82	-6.38	-7.25	-7.66	-7.93	-8.75
	15°S - 40°S	-2.15	-1.06	-3.04	-1.03	-4.77	-3.21
	40°S - 66°S	0.43	-2.78	0.86	-3.04	1.54	-5.03
Pacific Ocean	40°N - 66°N	-3.96	-4.87	-4.67	-5.18	4.73	1.02
	15°N - 40°N	2.33	2.04	2.33	2.03	3.17	1.71
	15°S - 15°N	-0.54	-0.88	0.94	-1.24	-0.14	-2.51
	15°S - 40°S	-7.93	-1.13	-8.26	-1.37	-7.13	-2.33
	40°S - 66°S	0.31	-3.06	0.86	-3.08	-0.36	-2.43
Indian Ocean	North of 15°S	0.09	-0.75	-0.09	-0.64	-0.41	-0.80
	15°N - 40°N	-2.03	-5.70	-2.57	-6.35	-2.89	-5.95
	40°N - 66°N	-5.37	4.97	-5.67	5.79	-4.31	5.95
Southern Ocean	66°S - 90°S	4.87	12.97	5.69	14.26	-13.58	14.05

452 is stronger or weaker differs per region (Table 2, Fig. 8 and Fig. 9). Interesting differ-
 453 ences are, for example, that TSB increases in the subpolar North Pacific and decreases
 454 in the Antarctic Ocean as a response to the strong AMOC weakening, but that the biomass
 455 of commercial species show the opposite response (i.e. a decrease and an increase, re-
 456 spectively) in SSP1-2.6. This effect occurs in regions surrounding the sea-ice edge. This
 457 suggests that lower trophic levels respond faster to sea ice changes resulting in the de-
 458 crease in TSB and TCB, while higher trophic levels respond slower resulting in a differ-
 459 ent response in total commercial biomass.

460 3.5 Role of AMOC weakening in EcoOcean

461 Total system (Fig. 7), consumer (Fig. 8), and commercial (Fig. 9), biomass all re-
 462 spond similar to the AMOC weakening (Fig. 6). Here we discuss the role of the AMOC
 463 weakening on total consumer biomass, and the mechanisms described also apply to to-
 464 tal system and commercial biomass. Total consumer biomass (Fig. 8) follows in most
 465 regions the patterns seen in changes in total phytoplankton biomass. This means that
 466 to first order, the effects of an AMOC weakening on marine ecosystems follow the same
 467 mechanisms as for total phytoplankton biomass, which is the combined effect of the mech-
 468 anisms present for the diazotrophs, diatoms and small phytoplankton. This means that
 469 the effects of an AMOC weakening affect marine ecosystems in a bottom up fashion by
 470 affecting the lowest trophic levels which through food web dynamics affect the entire ecosys-
 471 tem. There are a few regions that do not follow the patterns seen in total phytoplank-
 472 ton biomass, i.e. the Canary and Benguela Upwelling Systems, and the extension of the
 473 Gulf Stream. These are regions where a shift occurs in phytoplankton dominance, i.e.
 474 from small phytoplankton to diatoms in the Canary Upwelling System, and the other
 475 way around for the other two regions. These changes affect the food web dynamics in
 476 EcoOcean. In the Benguela Upwelling System and the surrounding ocean a decrease in
 477 total phytoplankton biomass is simulated in CESM2 (Fig. 5), but the surrounding oceans
 478 in EcoOcean show an increase in TCB (Fig. 8). Besides an increase in TCB, the sur-

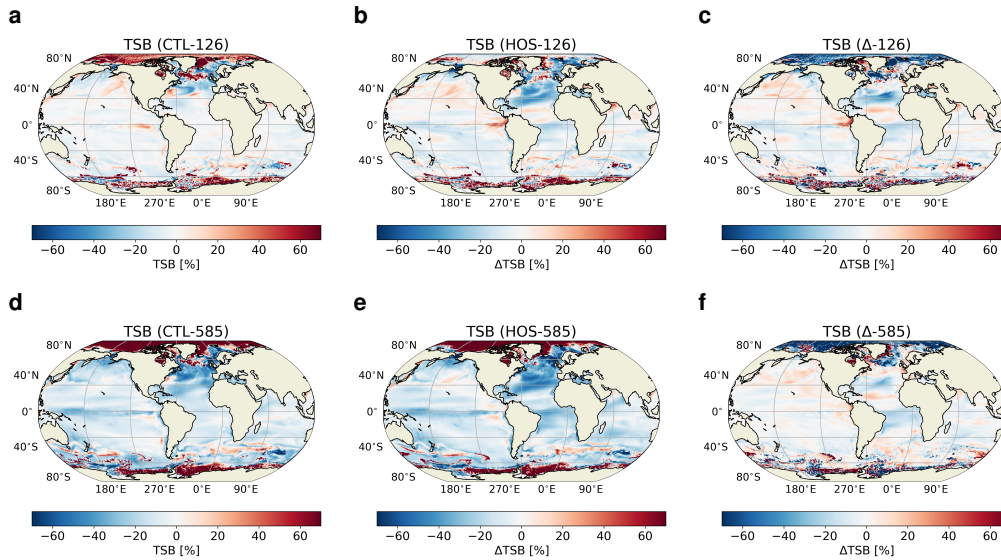


Figure 7. Relative changes averaged over 2095-2099 compared to 2016-2020 in % for Total System Biomass (TSB) in the CTL simulations (a, d), HOS simulations (b, e), and the difference between the two (c, f). (a-c) are for SSP1-2.6 and (d-f) are fore SSP5-8.5.

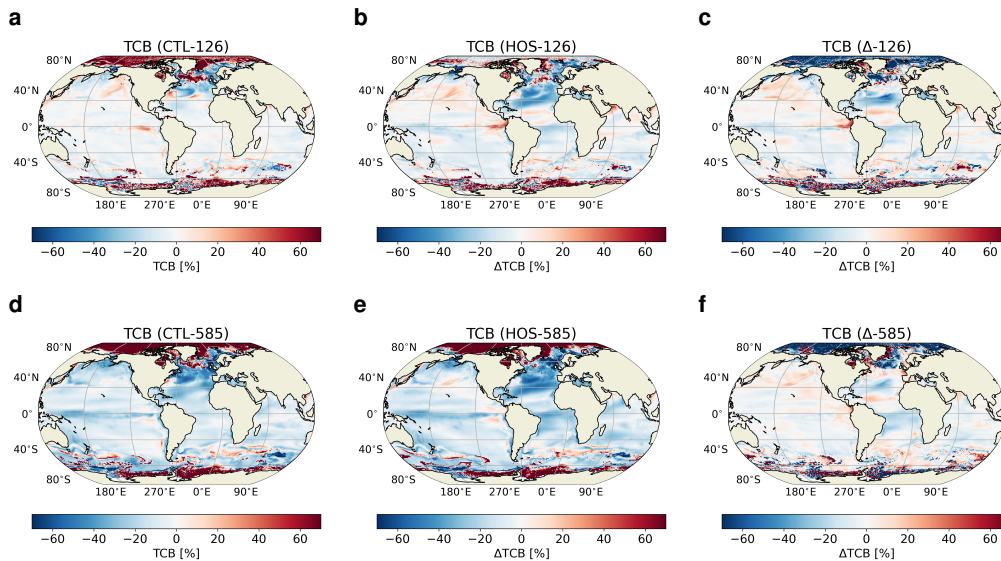


Figure 8. Relative changes averaged over 2095-2099 compared to 2016-2020 in % for Total Consumer Biomass (TCB) in the CTL simulations (a, d), HOS simulations (b, e), and the difference between the two (c, f). (a-c) are for SSP1-2.6 and (d-f) are fore SSP5-8.5.

479 rounding oceans also see an increase in both meso- and microzooplankton. Mesozooplankton
 480 (Fig. S22) are a central organism in the food web that feed on diatoms, diazotrophs
 481 and microzooplankton (Fig. S21) which predominantly feed on small phytoplankton. Since
 482 mesozooplankton have multiple food sources, they are able to increase their biomass even
 483 though diatom biomass is lost in this region. The reason why TCB follows mesozooplank-

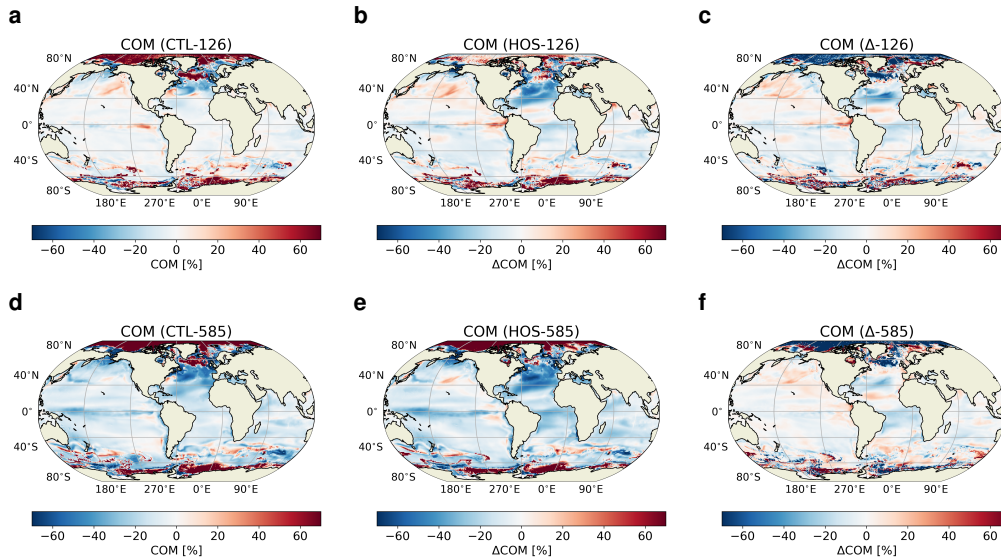


Figure 9. Relative changes averaged over 2095-2099 compared to 2016-2020 in % for commercial species (COM) in the CTL simulations (a, d), HOS simulations (b, e), and the difference between the two (c, f). (a-c) are for SSP1-2.6 and (d-f) are for SSP5-8.5.

484 ton biomass closely is that mesozooplankton have a central role in the ecosystem since
 485 they are preyed upon by 26 different functional groups, and often are the most impor-
 486 tant food source for these groups in EcoOcean. In the Canary Upwelling System, we see
 487 a strong increase in phytoplankton biomass due to an increase in diatom biomass over
 488 a loss of small phytoplankton biomass. This leads to an increase in large zooplankton
 489 (krill; Fig. S23), a small decrease in mesozooplankton and a large decrease in microzoo-
 490 plankton. In the Benguela Upwelling System similar mechanisms with opposite effects
 491 are present, and the changes in the food web dynamics lead to reduced TCB in this re-
 492 gion. In the extension of the Gulf Stream we find a strong decrease in diatom biomass
 493 in the HOS simulations, which is partly compensated for by small phytoplankton. How-
 494 ever, the net effect in this region is a strong decrease in total phytoplankton biomass.
 495 TCB does not follow this strong decrease in total phytoplankton biomass. This is be-
 496 cause the increase in small phytoplankton biomass, results in an increase in microzoo-
 497 plankton biomass. The mesozooplankton are consequently able to replace diatoms as a
 498 food source with microzooplankton as a food source.

499 4 Discussion

500 In this study we have looked at the effect of a strong weakening of the Atlantic Merid-
 501 ional Overturning Circulation (AMOC) on future global marine ecosystems under a low
 502 and high emission scenario. Fig. 10 provides an overview of how the AMOC weakening
 503 affects the climate system, ocean biogeochemistry and marine ecosystems. We see that
 504 the AMOC weakening has a large impact on the ocean state influencing ocean circula-
 505 tion, stratification and upwelling which leads to changes in the 3D nutrient fields. The
 506 changes in the nutrient fields directly affect the productivity and biomass of the three
 507 phytoplankton groups simulated in CESM2, i.e. the diazotrophs, diatoms and small phy-
 508 toplankton. The effects of the AMOC weakening on the phytoplankton cascade through
 509 the food web leading to a similar response in total consumer biomass as the response in
 510 total phytoplankton biomass. There are some regions that deviate from this overall re-

511 sponse. These regions typically see a shift in dominant phytoplankton group which causes
512 an adjustment in the abundance of the three different zooplankton groups in EcoOcean.
513 The mesozooplankton group is a central group in the food web that preys on both di-
514 atoms and microzooplankton that in turn prey on the small phytoplankton group. Through
515 this differential feeding, mesozooplankton do not directly follow the trend of total phy-
516 toplankton biomass in regions that observe a phytoplankton composition shift.

517 Overall, climate change causes a reduction in both total system and total consumer
518 biomass with a much stronger response in the high emission scenario. Similar changes
519 are seen in the commercial species, suggesting that these effects will also be felt in socio-
520 economic systems. The AMOC weakening leads to a stronger decrease in biomass in the
521 aggregated groups mentioned above. The responses in total system, consumer and com-
522 mercial biomass to an AMOC weakening are larger than the responses in total phyto-
523 plankton biomass, showing that the effect of the AMOC weakening is stronger on higher
524 trophic levels.

525 EcoOcean has previously been coupled to Earth System Model (ESM) simulations
526 using the GFDL and IPSL ESMs (Coll et al., 2020). Both ESMs show a different response
527 for TSB to the climate change and the CESM2 simulations result in again a different re-
528 sponse that lies between both the GFDL (relatively positive) and the IPSL (quite nega-
529 tive) responses. In FishMIP2 (Tittensor et al., 2021), EcoOcean is one of the more con-
530 servative marine ecosystem models and the only MEM with a complete, resilient food
531 web. Compared to these two studies (Coll et al., 2020; Tittensor et al., 2021), the results
532 presented here for TSB could be either more positive or negative when a different ESM
533 is used, and more extreme in biomass loss when a different MEM is used.

534 There is quite some work based on Earth System Models of Intermediate Complex-
535 ity (so-called EMICs) which generally focuses on longer timescales (i.e. multi-centennial
536 to multi-millennial). These studies show a wide range of possible responses in the ma-
537 rine carbon cycle (Zickfeld et al., 2008), but no clear analysis has been performed on ma-
538 rine ecosystems. Schmittner (2005) looks at the ecosystem response to an AMOC weak-
539 ening using a much simpler model than the models used in this study and suggests that
540 on long timescales an AMOC weakening results in a suppression of NPP in the Atlantic,
541 which is also what we find.

542 Since only one ESM and one MEM are used here, the results could be model de-
543 pendent. The most important forcing in EcoOcean is the total phytoplankton biomass
544 simulated in CESM2, and it would be very valuable to also use models with at least a
545 different biogeochemical module, and preferably a different ESM with a different ocean
546 component than CESM2. The spread in MEMs in FishMIP2 is generally smaller than
547 that of ESMs in CMIP6 (Tittensor et al., 2021), and therefore additional simulations with
548 different MEMs will provide less information than using different ESMs, but are valu-
549 able, nonetheless.

550 The results presented in this study hold implications for the efforts of mitigating
551 climate change, the management of marine ecosystems, and socio-economic systems. If
552 the AMOC strongly weakens, or even collapses in the coming century, marine ecosys-
553 tems are negatively affected. This comes on top of the generally negative effects that an-
554 thropogenic climate change and other human activities such as fisheries have on these
555 same ecosystems (Coll et al., 2020; Tittensor et al., 2021). We show that the AMOC weak-
556 ening on top of anthropogenic climate change can result in basin wide depletion of high
557 trophic level organisms, which can be also important for fisheries and food security. Pre-
558 vious studies have already stated that an AMOC weakening can affect societies through
559 large regional climate changes (van Westen et al., 2024; Brovkin et al., 2021). We show
560 here an additional pathway on how an AMOC weakening affects socio-economic systems
561 through a reduction in abundance of commercial species. Since fish is an essential source
562 of protein for millions of people (FAO, 2022), an AMOC weakening can have a disrupt-

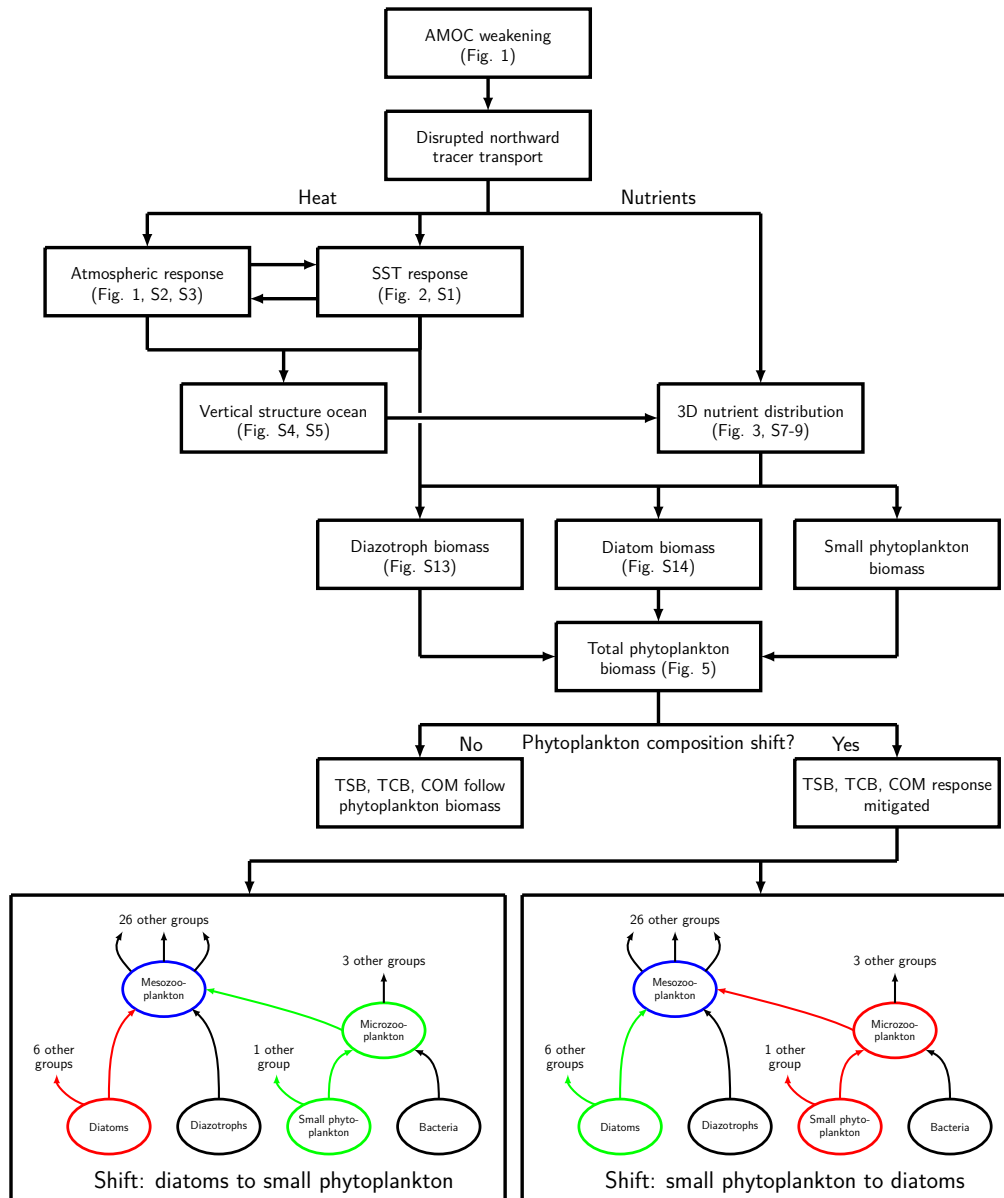


Figure 10. Summarizing figure showing in a simplified way how an AMOC weakening influences the climate system, ocean biogeochemistry and marine ecosystems. The diagrams at the bottom represent part of the food web in EcoOcean showing the response of the food web to a phytoplankton composition shift. The colors represent a decrease in biomass (red), an increase in biomass (green), and an unknown response (blue) in the mesozooplankton group.

563 tive effect on human societies. This is especially relevant since recent studies suggest we
 564 are approaching a tipping point for the AMOC (Ditlevsen & Ditlevsen, 2023; van Westen
 565 et al., 2024).

566 To conclude, in this study we have simulated a strong AMOC weakening using a
 567 low and high emission scenario in the CMIP6 state-of-the-art Earth System Model CESM2.

We forced a Marine Ecosystem Model, EcoOcean, with the CESM2 results to show the impact of an AMOC weakening on marine ecosystems. Both the low and high emission scenario show negative effects of the marine ecosystem, meaning that an AMOC weakening is an additional threat next to anthropogenic climate change. Another implication of our results is that tipping in the climate system can cascade over system boundaries to marine ecosystems, with possibly very negative effects on socio-economical systems.

5 Open Research

The scripts used for analysis and plotting, including the necessary datasets are saved in a repository: <https://doi.org/10.5281/zenodo.10891003> (Boot, Steenbeek, et al., 2024). In this repository also the most important output from the CESM2 and EcoOcean simulations is provided.

Acknowledgments

This study has been supported by the Netherlands Earth System Science Centre (NESSC), which is financially supported by the Ministry of Education, Culture and Science (OCW; Grant 024.002.001). A.A.B. and H.A.D. are also funded by the European Research Council through the ERC-AdG project TAOC (project 101055096). JS and MC acknowledge the European Union's Horizon 2020 research and innovation programme under grant agreement N°817578 (TRIATLAS) and the Spanish Ministry of Science and Innovation grant agreement N°PID2020-118097RB-I00 (ProOceans). MC acknowledges institutional support of the 'Severo Ochoa Centre of Excellence' accreditation (CEX2019-000928-S). The work of A.S.vdH. was also funded by the Dutch Research Council (NWO) through the NWO-Vici project 'Interacting climate tipping elements: When does tipping cause tipping?' (project VI.C.202.081). The authors want to thank Michael Kliphuis (IMAU, Utrecht University) for performing the CESM2 simulations, which were performed at SURFsara in Amsterdam on the Dutch Supercomputer Snellius under NWO-SURF project 17239.

References

- Ahrens, R. N. M., Walters, C. J., & Christensen, V. (2012). Foraging arena theory. *Fish and Fisheries*, *13*(1), 41–59. doi: <https://doi.org/10.1111/j.1467-2979.2011.00432.x>
- Boot, A. A., Steenbeek, J., Coll, M., von der Heydt, A. S., & Dijkstra, H. A. (2024, mar). *dboot0016/EF2024-CESM2-EcoOcean: v1.1*. Zenodo. doi: 10.5281/zenodo.10891003
- Boot, A. A., von der Heydt, A. S., & Dijkstra, H. A. (2023). Effect of Plankton Composition Shifts in the North Atlantic on Atmospheric pCO₂. *Geophysical Research Letters*, *50*(2), e2022GL100230. doi: <https://doi.org/10.1029/2022GL100230>
- Boot, A. A., von der Heydt, A. S., & Dijkstra, H. A. (2024). Response of atmospheric pCO₂ to a strong AMOC weakening under low and high emission scenarios. *Under review at Climate Dynamics*.
- Boucher, O., Servonnat, J., Albright, A. L., Aumont, O., Balkanski, Y., Bastrikov, V., ... Vuichard, N. (2020). Presentation and Evaluation of the IPSL-CM6A-LR Climate Model. *Journal of Advances in Modeling Earth Systems*, *12*(7), e2019MS002010. doi: <https://doi.org/10.1029/2019MS002010>
- Breitburg, D., Levin, L. A., Oschlies, A., Grégoire, M., Chavez, F. P., Conley, D. J., ... Zhang, J. (2018). Declining oxygen in the global ocean and coastal waters. *Science*, *359*(6371), eaam7240. doi: 10.1126/science.aam7240
- Brovkin, V., Brook, E., Williams, J. W., Bathiany, S., Lenton, T. M., Barton, M., ... Yu, Z. (2021). Past abrupt changes, tipping points and cascad-

- ing impacts in the Earth system. *Nature Geoscience*, *14*(8), 550–558. doi: 10.1038/s41561-021-00790-5
- Caesar, L., Rahmstorf, S., Robinson, A., Feulner, G., & Saba, V. (2018). Observed fingerprint of a weakening Atlantic Ocean overturning circulation. *Nature*, *556*(7700), 191–196. doi: 10.1038/s41586-018-0006-5
- Christensen, V., Coll, M., Buszowski, J., Cheung, W. W. L., Frölicher, T., Steenbeek, J., ... Walters, C. J. (2015). The global ocean is an ecosystem: simulating marine life and fisheries. *Global Ecology and Biogeography*, *24*(5), 507–517. doi: <https://doi.org/10.1111/geb.12281>
- Christensen, V., Coll, M., Steenbeek, J., Buszowski, J., Chagaris, D., & Walters, C. J. (2014). Representing Variable Habitat Quality in a Spatial Food Web Model. *Ecosystems*, *17*(8), 1397–1412. doi: 10.1007/s10021-014-9803-3
- Coll, M., Steenbeek, J., Pennino, M. G., Buszowski, J., Kaschner, K., Lotze, H. K., ... Christensen, V. (2020). Advancing Global Ecological Modeling Capabilities to Simulate Future Trajectories of Change in Marine Ecosystems. *Frontiers in Marine Science*, *7*. doi: 10.3389/fmars.2020.567877
- Danabasoglu, G. (2019). *NCAR CESM2 model output prepared for CMIP6 CMIP esm-hist*. Earth System Grid Federation. doi: 10.22033/ESGF/CMIP6.7575
- Danabasoglu, G., Lamarque, J.-F., Bacmeister, J., Bailey, D. A., DuVivier, A. K., Edwards, J., ... Strand, W. G. (2020). The Community Earth System Model Version 2 (CESM2). *Journal of Advances in Modeling Earth Systems*, *12*(2), e2019MS001916. doi: <https://doi.org/10.1029/2019MS001916>
- Diaz, R. J., & Rosenberg, R. (2008). Spreading Dead Zones and Consequences for Marine Ecosystems. *Science*, *321*(5891), 926–929. doi: 10.1126/science.1156401
- Ditlevsen, P., & Ditlevsen, S. (2023). Warning of a forthcoming collapse of the Atlantic meridional overturning circulation. *Nature Communications*, *14*(1), 4254.
- Doney, S. C., Ruckelshaus, M., Emmett Duffy, J., Barry, J. P., Chan, F., English, C. A., ... Talley, L. D. (2012). Climate Change Impacts on Marine Ecosystems. *Annual Review of Marine Science*, *4*(1), 11–37. doi: 10.1146/annurev-marine-041911-111611
- Dunne, J. P., Horowitz, L. W., Adcroft, A. J., Ginoux, P., Held, I. M., John, J. G., ... Zhao, M. (2020). The GFDL Earth System Model Version 4.1 (GFDL-ESM 4.1): Overall Coupled Model Description and Simulation Characteristics. *Journal of Advances in Modeling Earth Systems*, *12*(11), e2019MS002015. doi: <https://doi.org/10.1029/2019MS002015>
- Eyring, V., Bony, S., Meehl, G. A., Senior, C. A., Stevens, B., Stouffer, R. J., & Taylor, K. E. (2016, may). Overview of the Coupled Model Intercomparison Project Phase 6 (CMIP6) experimental design and organization. *Geosci. Model Dev.*, *9*(5), 1937–1958. doi: 10.5194/gmd-9-1937-2016
- FAO. (2022). *The state of world fisheries and aquaculture 2022*. FAO.
- Forget, G., & Ferreira, D. (2019). Global ocean heat transport dominated by heat export from the tropical Pacific. *Nature Geoscience*, *12*(5), 351–354. doi: 10.1038/s41561-019-0333-7
- Gattuso, J.-P., Magnan, A., Billé, R., Cheung, W. W. L., Howes, E. L., Joos, F., ... Turley, C. (2015). Contrasting futures for ocean and society from different anthropogenic CO₂ emissions scenarios. *Science*, *349*(6243), aac4722. doi: 10.1126/science.aac4722
- Henson, S. A., Cael, B. B., Allen, S. R., & Dutkiewicz, S. (2021). Future phytoplankton diversity in a changing climate. *Nature Communications*, *12*(1), 5372. doi: 10.1038/s41467-021-25699-w
- Henson, S. A., Laufkötter, C., Leung, S., Giering, S. L. C., Palevsky, H. I., & Cavan, E. L. (2022). Uncertain response of ocean biological carbon export in a changing world. *Nature Geoscience*, *15*(4), 248–254. doi:

- 672 10.1038/s41561-022-00927-0
673 Hoegh-Guldberg, O., & Bruno, J. F. (2010). The Impact of Climate Change on the
674 World's Marine Ecosystems. *Science*, *328*(5985), 1523–1528. doi: 10.1126/
675 science.1189930
676 Hunke, E. C., Lipscomb, W. H., Turner, A. K., Jeffrey, N., & Elliott, S. (2015).
677 *CICE: The Los Alamos Sea Ice Model documentation and software user's man-*
678 *ual, version 5.1. Doc* (Tech. Rep.). LA-CC-06-012, 116 pp., <http://www.ccpo.>
679 [edu](http://www.ccpo.edu).
680 IPCC. (2022). *The ocean and cryosphere in a changing climate*. Cambridge, Eng-
681 land: Cambridge University Press.
682 Ito, T., & Follows, M. J. (2005). Preformed phosphate, soft tissue pump and atmo-
683 spheric CO₂. *Journal of Marine Research*, *63*(4), 813–839. doi: doi:10.1357/
684 0022240054663231
685 Kwiatkowski, L., Torres, O., Bopp, L., Aumont, O., Chamberlain, M., Christian,
686 J. R., . . . Ziehn, T. (2020). Twenty-first century ocean warming, acidifica-
687 tion, deoxygenation, and upper-ocean nutrient and primary production decline
688 from CMIP6 model projections. *Biogeosciences*, *17*(13), 3439–3470. doi:
689 10.5194/bg-17-3439-2020
690 Lawrence, D. M., Fisher, R. A., Koven, C. D., Oleson, K. W., Swenson, S. C., Bo-
691 nan, G., . . . Zeng, X. (2019, dec). The Community Land Model Version 5:
692 Description of New Features, Benchmarking, and Impact of Forcing Uncer-
693 tainty. *Journal of Advances in Modeling Earth Systems*, *11*(12), 4245–4287.
694 doi: <https://doi.org/10.1029/2018MS001583>
695 Lenton, T. M., Held, H., Kriegler, E., Hall, J. W., Lucht, W., Rahmstorf, S., &
696 Schellnhuber, H. J. (2008). Tipping elements in the Earth's climate system.
697 *Proceedings of the National Academy of Sciences*, *105*(6), 1786–1793. doi:
698 10.1073/pnas.0705414105
699 Liu, X., Battisti, D. S., & Donohoe, A. (2017). Tropical Precipitation and Cross-
700 Equatorial Ocean Heat Transport during the Mid-Holocene. *Journal of Cli-*
701 *mate*, *30*(10), 3529–3547. doi: <https://doi.org/10.1175/JCLI-D-16-0502.1>
702 Long, M. C., Moore, J. K., Lindsay, K., Levy, M., Doney, S. C., Luo, J. Y., . . .
703 Sylvester, Z. T. (2021). Simulations With the Marine Biogeochemistry Li-
704 brary (MARBL). *Journal of Advances in Modeling Earth Systems*, *13*(12),
705 e2021MS002647. doi: <https://doi.org/10.1029/2021MS002647>
706 Lotze, H. K., Tittensor, D. P., Bryndum-Buchholz, A., Eddy, T. D., Cheung,
707 W. W. L., Galbraith, E. D., . . . Worm, B. (2019). Global ensemble projections
708 reveal trophic amplification of ocean biomass declines with climate change.
709 *Proceedings of the National Academy of Sciences*, *116*(26), 12907–12912. doi:
710 10.1073/pnas.1900194116
711 Manral, D., Iovino, D., Jaillon, O., Masina, S., Sarmiento, H., Iudicone, D., . . .
712 van Sebille, E. (2023). Computing marine plankton connectivity un-
713 der thermal constraints. *Frontiers in Marine Science*, *10*. doi: 10.3389/
714 fmars.2023.1066050
715 Martell, S. J. D., Essington, T. E., Lessard, B., Kitchell, J. F., Walters, C. J., &
716 Boggs, C. H. (2005). Interactions of productivity, predation risk, and fish-
717 ing effort in the efficacy of marine protected areas for the central Pacific.
718 *Canadian Journal of Fisheries and Aquatic Sciences*, *62*(6), 1320–1336. doi:
719 10.1139/f05-114
720 McKay, D. I. A., Staal, A., Abrams, J. F., Winkelmann, R., Sakschewski, B., Lo-
721 riani, S., . . . Lenton, T. M. (2022). Exceeding 1.5°C global warming
722 could trigger multiple climate tipping points. *Science*, *377*(6611), eabn7950.
723 doi: 10.1126/science.abn7950
724 Moore, C. M., Mills, M. M., Arrigo, K. R., Berman-Frank, I., Bopp, L., Boyd,
725 P. W., . . . Ulloa, O. (2013). Processes and patterns of oceanic nutrient
726 limitation. *Nature Geoscience*, *6*(9), 701–710. doi: 10.1038/ngeo1765

- 727 Moore, J. K., Doney, S. C., Kleypas, J. A., Glover, D. M., & Fung, I. Y. (2001). An
728 intermediate complexity marine ecosystem model for the global domain. *Deep*
729 *Sea Research Part II: Topical Studies in Oceanography*, 49(1), 403–462. doi:
730 [https://doi.org/10.1016/S0967-0645\(01\)00108-4](https://doi.org/10.1016/S0967-0645(01)00108-4)
- 731 Moore, J. K., Doney, S. C., & Lindsay, K. (2004, dec). Upper ocean ecosystem
732 dynamics and iron cycling in a global three-dimensional model. *Global Biogeo-*
733 *chemical Cycles*, 18(4). doi: <https://doi.org/10.1029/2004GB002220>
- 734 Moore, J. K., Lindsay, K., Doney, S. C., Long, M. C., & Misumi, K. (2013). Marine
735 Ecosystem Dynamics and Biogeochemical Cycling in the Community Earth
736 System Model [CESM1(BGC)]: Comparison of the 1990s with the 2090s under
737 the RCP4.5 and RCP8.5 Scenarios. *Journal of Climate*, 26(23), 9291–9312.
738 doi: <https://doi.org/10.1175/JCLI-D-12-00566.1>
- 739 Orihuela-Pinto, B., England, M. H., & Taschetto, A. S. (2022). Interbasin and in-
740 terhemispheric impacts of a collapsed Atlantic Overturning Circulation. *Nature*
741 *Climate Change*, 12(6), 558–565. doi: 10.1038/s41558-022-01380-y
- 742 Sampaio, E., Santos, C., Rosa, I. C., Ferreira, V., Pörtner, H.-O., Duarte, C. M.,
743 ... Rosa, R. (2021). Impacts of hypoxic events surpass those of future ocean
744 warming and acidification. *Nature Ecology & Evolution*, 5(3), 311–321. doi:
745 10.1038/s41559-020-01370-3
- 746 Sanders, R., Henson, S. A., Koski, M., De La Rocha, C. L., Painter, S. C., Poul-
747 ton, A. J., ... Martin, A. P. (2014). The Biological Carbon Pump
748 in the North Atlantic. *Progress in Oceanography*, 129, 200–218. doi:
749 <https://doi.org/10.1016/j.pocean.2014.05.005>
- 750 Schmittner, A. (2005). Decline of the marine ecosystem caused by a reduction in the
751 Atlantic overturning circulation. *Nature*, 434(7033), 628–633. doi: 10.1038/
752 nature03476
- 753 Smale, D. A., Wernberg, T., Oliver, E. C. J., Thomsen, M., Harvey, B. P., Straub,
754 S. C., ... Moore, P. J. (2019). Marine heatwaves threaten global biodiversi-
755 ty and the provision of ecosystem services. *Nature Climate Change*, 9(4),
756 306–312. doi: 10.1038/s41558-019-0412-1
- 757 Smith, R., Jones, P. W., Briegleb, P. A., Bryan, O., Danabasoglu, G., Dennis,
758 M. L., ... Yeager, S. G. (2010). The Parallel Ocean Program (POP) refer-
759 ence manual: Ocean component of the Community Climate System Model
760 (CCSM)..
- 761 Tagliabue, A., Kwiatkowski, L., Bopp, L., Butenschön, M., Cheung, W., Lengaigne,
762 M., & Vialard, J. (2021). Persistent Uncertainties in Ocean Net Primary
763 Production Climate Change Projections at Regional Scales Raise Challenges
764 for Assessing Impacts on Ecosystem Services. *Frontiers in Climate*, 3. doi:
765 10.3389/fclim.2021.738224
- 766 Tittensor, D. P., Eddy, T. D., Lotze, H. K., Galbraith, E. D., Cheung, W., Barange,
767 M., ... Walker, N. D. (2018). A protocol for the intercomparison of marine
768 fishery and ecosystem models: Fish-MIP v1.0. *Geoscientific*
769 *Model Development*, 11(4), 1421–1442. doi: 10.5194/gmd-11-1421-2018
- 770 Tittensor, D. P., Novaglio, C., Harrison, C. S., Heneghan, R. F., Barrier, N.,
771 Bianchi, D., ... Blanchard, J. L. (2021). Next-generation ensemble pro-
772 jections reveal higher climate risks for marine ecosystems. *Nature Climate*
773 *Change*, 11(11), 973–981. doi: 10.1038/s41558-021-01173-9
- 774 van Westen, R. M., & Dijkstra, H. A. (2023a). Asymmetry of AMOC Hysteresis in a
775 State-Of-The-Art Global Climate Model. *Geophysical Research Letters*, 50(22),
776 e2023GL106088. doi: <https://doi.org/10.1029/2023GL106088>
- 777 van Westen, R. M., & Dijkstra, H. A. (2023b). Persistent Climate Model Biases in
778 the Atlantic Ocean’s Freshwater Transport. *EGUsphere*, 2023, 1–29. doi: 10
779 .5194/egusphere-2023-1502
- 780 van Westen, R. M., Kliphuis, M., & Dijkstra, H. A. (2024). Physics-based early
781 warning signal shows that AMOC is on tipping course. *Science Advances*,

- 782 10(6), eadk1189. doi: 10.1126/sciadv.adk1189
- 783 Walters, C. J., & Juanes, F. (1993). Recruitment Limitation as a Consequence
784 of Natural Selection for Use of Restricted Feeding Habitats and Predation
785 Risk Taking by Juvenile Fishes. *Canadian Journal of Fisheries and Aquatic*
786 *Sciences*, 50(10), 2058–2070. doi: 10.1139/f93-229
- 787 Weijer, W., Cheng, W., Drijfhout, S. S., Fedorov, A. V., Hu, A., Jackson, L. C., ...
788 Zhang, J. (2019, aug). Stability of the Atlantic Meridional Overturning Cir-
789 culation: A Review and Synthesis. *Journal of Geophysical Research: Oceans*,
790 124(8), 5336–5375. doi: <https://doi.org/10.1029/2019JC015083>
- 791 Weijer, W., Cheng, W., Garuba, O. A., Hu, A., & Nadiga, B. T. (2020, jun).
792 CMIP6 Models Predict Significant 21st Century Decline of the Atlantic
793 Meridional Overturning Circulation. *Geophysical Research Letters*, 47(12),
794 e2019GL086075. doi: <https://doi.org/10.1029/2019GL086075>
- 795 Worthington, E. L., Moat, B. I., Smeed, D. A., Mecking, J. V., Marsh, R., & Mc-
796 Carthy, G. D. (2021). A 30-year reconstruction of the Atlantic meridional
797 overturning circulation shows no decline. *Ocean Science*, 17(1), 285–299. doi:
798 10.5194/os-17-285-2021
- 799 Zickfeld, K., Eby, M., & Weaver, A. J. (2008, sep). Carbon-cycle feedbacks of
800 changes in the Atlantic meridional overturning circulation under future at-
801 mospheric CO₂. *Global Biogeochemical Cycles*, 22(3). doi: [https://doi.org/](https://doi.org/10.1029/2007GB003118)
802 10.1029/2007GB003118